Predicting euphotic-depth-integrated chlorophyll-a from discrete-depth and satellite-observable chlorophyll-a off central California

Article *in* Journal of Geophysical Research Atmospheres · May 2012

DOI: 10.1029/2011JC007322

CITATIONS
13

READS
169

3 authors, including:

Sergey Frolov
United States Naval Research Laboratory
36 PUBLICATIONS **390** CITATIONS

SEE PROFILE

John Ryan
Monterey Bay Aquarium Research Institute
129 PUBLICATIONS **5,387** CITATIONS

SEE PROFILE

Predicting euphotic-depth-integrated chlorophyll-*a* from discrete-depth and satellite-observable chlorophyll-*a* off central California

Sergey Frolov,[1,2] J. P. Ryan,[1] and F. P. Chavez[1]

Received 27 May 2011; revised 19 March 2012; accepted 14 April 2012; published 26 May 2012.

[1] Predicting water column integrated phytoplankton biomass from near-surface measurements has been an important effort in marine ecological research, particularly since the advent of satellite remote sensing of ocean color. Quantitative relationships between chlorophyll-*a* concentrations (Chl-*a*) at the surface and its depth-integrated magnitude have thus far only been developed for open-ocean waters. Here we develop and test for the first time an extension of open-ocean relationships into ocean-margin waters, specifically the highly productive and variable eastern boundary upwelling ecosystem off the central California coast. This region was chosen because of the unique availability of a 30-year record of ship-based Chl-*a* profiles measured using consistent methods. The extended relationship allows accurate prediction of integrated biomass from surface measurements. Further, we develop a new set of relationships for predicting the depth-integrated Chl-*a* from Chl-*a* measured over a range of discrete depths (i.e., as measured by fluorometers on moorings). The newly developed relationships are tested against 15,000 fluorometric Chl-*a* profiles obtained from an autonomous underwater vehicle. Surprisingly, the relationship between surface Chl-*a* and depth-integrated Chl-*a* holds for profiles with high concentrations of Chl-*a* in persistent subsurface thin phytoplankton layers (layers <3 m thick and located below the first optical depth). The results have implications for monitoring of algal blooms and for quantifying ocean primary productivity from satellite observations of ocean color.

Citation: Frolov, S., J. P. Ryan, and F. P. Chavez (2012), Predicting euphotic-depth-integrated chlorophyll-*a* from discrete-depth and satellite-observable chlorophyll-*a* off central California, *J. Geophys. Res.*, *117*, C05042, doi:10.1029/2011JC007322.

1. Introduction

[2] Euphotic-depth-integrated chlorophyll-*a* (Chl-*a*) is a fundamental indicator of variability in primary production, supply of energy to higher trophic levels, and onset of potentially harmful algal blooms. Satellite remote sensing of ocean color and moored deployments of in situ Chl-*a* fluorometers describe spatial and temporal variability in phytoplankton abundance. However, interpretation of the near-surface measurements from satellites and discrete-depth measurements from moorings requires knowledge of the relationship between these vertically sparse measurements and euphotic-depth-integrated Chl-*a*. In the open ocean, *Morel and Berthon* [1989] used an extensive data set of Chl-*a* profiles to establish that surface measurements of Chl-*a*—as for example estimated from satellite remote sensing of ocean color—can be used as a predictor of the depth-integrated Chl-*a*. Later this seminal relationship was further refined by *Uitz et al.* [2006] using more complete and updated data sets. However, it has not been established yet if similar relationships exist in the coastal ocean.

[3] Although coastal waters comprise only a small part of the world ocean surface area (8%), they account for a disproportionally large part of the world fishery catch (up to 90%) and primary production (20–30%) [*Pauly and Christensen*, 1995]. Thus, accurate prediction of phytoplankton variability in coastal waters is particularly valuable to marine ecological research and informed management of living resources. The data sets used by *Morel and Berthon* [1989] and later used by *Uitz et al.* [2006] lacked adequate coverage in highly productive coastal areas. Testing the extension of open-ocean relationships to productive coastal waters is long overdue. In this article, we present the first extension of the relationships of *Morel and Berthon* [1989] and *Uitz et al.* [2006] to a coastal ecosystem. The focus of this study is on the central part of the California Current upwelling ecosystem (CCCUE)—a highly productive ecosystem off the coast of central and northern California (from 34°N to 40°N). Our study is based on an extensive, multidecadal time series of Chl-*a* measurements.

[4] Several aspects of circulation and phytoplankton ecology in the CCCUE are distinct from that of the open ocean and,

[1]Monterey Bay Aquarium Research Institute, Moss Landing, California, USA.
[2]Naval Research Laboratory, University Corporation for Atmospheric Research, Monterey, California, USA.

Corresponding author: S. Frolov, Naval Research Laboratory, University Corporation for Atmospheric Research, 7 Grace Hopper Av., Monterey, CA 93943, USA. (frolovsa@gmail.com)

0148-0227/12/2011JC007322

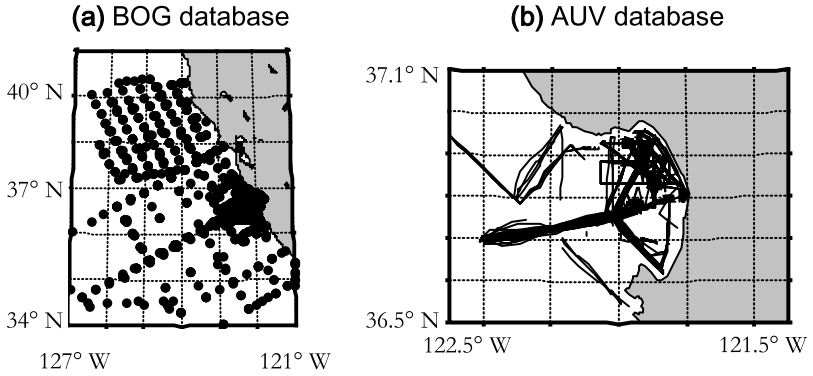

Figure 1. Distribution of samples in the (a) BOG database and (b) AUV database.

hence, may preclude application of the empirical open-ocean relationships to the CCCUE waters. These factors include coastal upwelling, higher phytoplankton biomass in the CCCUE waters, active swimming behavior of coastal dinoflagellates [*Cullen and Horrigan*, 1981; *Kiefer and Lasker*, 1975; *Ryan et al.*, 2010], and occurrence of persistent subsurface thin phytoplankton layers [*Cowles et al.*, 1998; *McManus et al.*, 2008; *Sullivan et al.*, 2010b]. Unlike the intermittent layering that is often observed in Chl-*a* fluorescence profiles [*Derenbach et al.*, 1979], thin layers in Monterey Bay are coherent over large spatial areas (100 m to ~10 km [*Ryan et al.*, 2010]), persist over extended periods of time (up to 7 days [*McManus et al.*, 2008]), and, when present, accumulate a considerable part of the integrated water column biomass (an average of 33–47% [*Sullivan et al.*, 2010a]). Previous studies by *Morel and Berthon* [1989] and *Uitz et al.* [2006] did not consider the effect of such persistent thin layers on the relationship between surface and depth-integrated Chl-*a.* Examination of thin layer effects requires resolution of water column chlorophyll at higher vertical resolution than ship surveys with Niskin bottles can provide. For this purpose, we use an extensive data set (~15,000 profiles) of Chl-*a* fluorescence profiles with a vertical resolution of 0.1 m to examine the effect of thin layers on the relationship between the surface and the depth-integrated Chl-*a.*

[5] The objectives of this study are to: (1) extend the predictive relationship between surface and depth-integrated Chl-*a* of *Uitz et al.* [2006] to highly productive waters of the CCCUE, (2) develop relationships for prediction of depth-integrated Chl-*a* from discrete-depth measurements of Chl-*a*, (3) test if the presence of thin-layer-peaks in Chl-*a* profiles affect predictability of depth-integrated Chl-*a*, and (4) determine the optimal depth for prediction of depth-integrated Chl-*a* from discrete-depth measurement.

2. Data Sets Used

2.1. BOG Data Set of Ship-Based Profiles

[6] The Biological Oceanography Group (BOG) data set (Figure 1a) consisted of ~2,800 discrete-depth Chl-*a* profiles that were obtained using traditional ship-based CTD surveys. Chl-*a* concentrations were determined from extracted Chl-*a* samples using the fluorometric method [*Pennington and Chavez*, 2000]. The data set extended from 1980 to 2010. Most of the BOG samples were collect off the continental shelf, with the median bottom depth of ~1500 m. Profiles shallower than the euphotic depth were removed from the data set. We used this data set to determine relationships that predicted euphotic-depth-integrated $\langle \text{Chl-}a \rangle_{\text{zeu}}$ values based on first-optical-depth-averaged $[\text{Chl-}a]_{\text{zpd}}$ and fixed-depth $[\text{Chl-}a]_{\text{z}}$ measurements.

[7] To limit a much larger BOG database to samples collected off the coast of central California, we defined the CCCUE samples as samples collected between Cape Mendocino and Pt. Conception and within 500 km from shore. We chose the 500 km distance by comparing the surface Chl-*a* values collected in the CCCUE region with the surface Chl-*a* values collected in the ocean gyre along a transact from

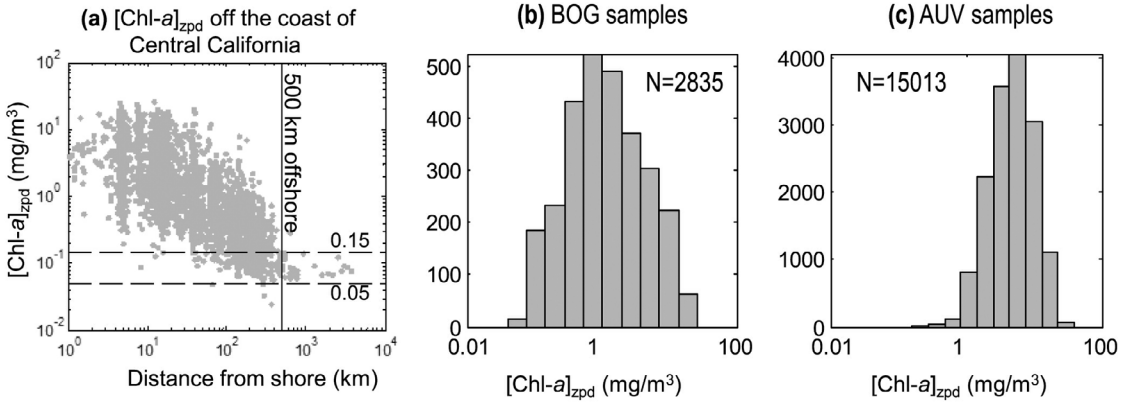

Figure 2. Distribution of $[\text{Chl-}a]_{\text{zpd}}$ (a) off the coast of central California as a function of distance from shore, (b) in the BOG database, and (c) in the AUV database.

Monterey Bay to Hawaii. Figure 2a shows that the range of observed surface Chl-*a* values declined sharply at 500 km distance to a range commonly found in samples collected further offshore in the ocean gyre (0.05–0.15 mg/m^3).

[8] Unlike the database previously used by *Uitz et al.* [2006], the BOG database includes a large number of profiles in high Chl-*a* waters (Figure 2b). For example, the *Uitz et al.* [2006] database had only 78 profiles with surface Chl-*a* values greater than 1 mg/m^3 (maximum value of 5 mg/m^3). In contrast, the new database has ~1500 profiles in this category (maximum value of 26 mg/m^3).

2.2. AUV Data Set of High-Resolution Florescence Profiles

[9] The Autonomous Underwater Vehicle (AUV) data set (Figure 1b) consisted of ~15,000 Chl-*a* fluorescence profiles with the vertical resolution of 0.1 m. Chl-*a* fluorescence was measured using a HOBI Labs HS2 sensor deployed on board of MBARI's Dorado AUV. The fluorometer was calibrated annually by the manufacturer to output accurate engineering units, which were then cross-calibrated to Chl-*a* units during an intensive field campaign [*Ryan et al.*, 2010]. Most of the AUV samples were collect on the continental shelf with the median bottom depth of 78 m. Profiles shallower than the euphotic depth were removed from the data set. This data set, extending from 2003 to 2010, was used to test the relationships established using the BOG database and to study the effects of thin layers on $\langle \text{Chl-}a \rangle_{\text{zeu}}$ predictability.

[10] There were three major differences between AUV and BOG data sets:

[11] 1. Unlike the extracted Chl-*a* measurements in the BOG data set, the in situ fluorescence-based measurements in the AUV data set can underestimate Chl-*a* due to photochemical quenching of Chl-*a* fluorescence at high light levels. However, this possible effect was reduced in our data set because a large portion (~70%) of the AUV profiles was collected at night or during evening and morning hours.

[12] 2. Unlike the BOG data that were collected over a wide range of conditions up to 500 km offshore, the AUV data were collected inside of the Monterey Bay, within 20 km from shore. As a result, AUV data set had higher Chl-*a* concentrations (compare histograms in Figures 2b and 2c).

[13] 3. Unlike the BOG data of extracted chlorophyll at discrete depths, the high-resolution AUV profiles provided sampling of thin layers, which are known to be present inside of Monterey Bay.

3. Methods

3.1. Depth-Integrated Quantities

[14] To relate surface Chl-*a* concentrations to depth-integrated Chl-*a*, we followed the *Uitz et al.* [2006] description of the original method developed by *Morel and Berthon* [1989]. To describe depth-integrated Chl-*a* content, we computed euphotic-depth-integrated Chl-*a* concentrations ($\langle \text{Chl-}a \rangle_{\text{zeu}}$) and euphotic-depth-averaged concentrations ($[\text{Chl-}a]_{\text{zeu}}$) as

$$\langle \text{Chl-}a \rangle_{zeu} = \int_0^{Z_{eu}} [\text{Chl-}a]_z dz \tag{1}$$

and

$$[\text{Chl-}a]_{zeu} = (Z_{eu})^{-1} \langle \text{Chl-}a \rangle_{zeu}, \tag{2}$$

where $[\text{Chl-}a]_z$ is the concentration of Chl-*a* at discrete depth z, and Z_{eu} is the euphotic depth at which light intensity is 1% of the surface value. Z_{eu} was not measured directly and was computed based on light extinction coefficients of pure water and Chl-*a* [*Morel and Maritorena*, 2001, equation (6)]. To describe the Chl-*a* concentrations measurable by the satellite, we followed *Uitz et al.* [2006] and averaged Chl-*a* concentration over the first optical depth $Z_{\text{pd}} = Z_{\text{eu}}/4.6$

$$[\text{Chl-}a]_{zpd} = \left(Z_{pd}\right)^{-1} \int_0^{Z_{pd}} [\text{Chl-}a]_z dz. \tag{3}$$

3.2. Regression Relationships and Error Statistics

[15] To quantify the nonlinear relationship between $\langle \text{Chl-}a \rangle_{\text{zeu}}$ and $[\text{Chl-}a]_{\text{zpd}}$ or $[\text{Chl-}a]_{\text{z}}$, we used the power law regression

$$\widehat{\langle \text{Chl-}a \rangle}_{zeu} = A[\text{Chl-}a]_z^B, \tag{4}$$

where A and B are the intercept and the slope of the linear regression estimated from the log-log transformed data, and $\widehat{\langle \text{Chl-}a \rangle}_{zeu}$ is the predicted value of $\langle \text{Chl-}a \rangle_{zeu}$. Similar to *Morel and Berthon* [1989], we fit two separate regression lines: one above and one below the 1 mg/m^3 threshold. In this paper we estimate regression parameters in equation (4) for profiles in stratified waters only (where mixed layer depth Z_{mld} is less than the euphotic depth Z_{eu}) because less than 5% of the profiles in the CCCUE region were classified as mixed ($Z_{\text{mld}} > Z_{\text{eu}}$). We computed the mixed layer depth Z_{mld} from temperature that accompanied our Chl-*a* data, using method described in *Lorbacher et al.* [2006].

[16] The relationship between the predictor and the predictant in equation (4) is linear in the log-log space; hence, it is appropriate to compute the following R^2 statistics

$$R^2 = 1 - \frac{\text{var}\left[\log_{10}\left(\widehat{\langle \text{Chl-}a \rangle}_{zeu}\right) - \log_{10}\left(\langle \text{Chl-}a \rangle_{zeu}\right)\right]}{\text{var}\left[\log_{10}\left(\langle \text{Chl-}a \rangle_{zeu}\right)\right]}. \tag{5}$$

[17] Equation (5) highlights the fact that errors in the log-log plots in Figure 3 are the ratios rather than the differences between the predicted and measured $\langle \text{Chl-}a \rangle_{\text{zeu}}$. To intercompare the R^2 values from different data sets, the variance in the denominator was computed for the combined AUV and BOG data sets.

[18] To quantify absolute error for the log-log regression, we computed the root mean square error (RMSE) of the model as

$$RMSE = 10\text{^}\sqrt{mean\left[\log_{10}\left(\widehat{\langle \text{Chl-}a \rangle}_{zeu}\right) - \log_{10}\left(\langle \text{Chl-}a \rangle_{zeu}\right)^2\right]}. \tag{6}$$

[19] The resulting RMSE statistics express error as the average number of times the predicted value was larger or smaller than the observed value. For example, RMSE of 1 means perfect prediction; RMSE of 1.5 means that model

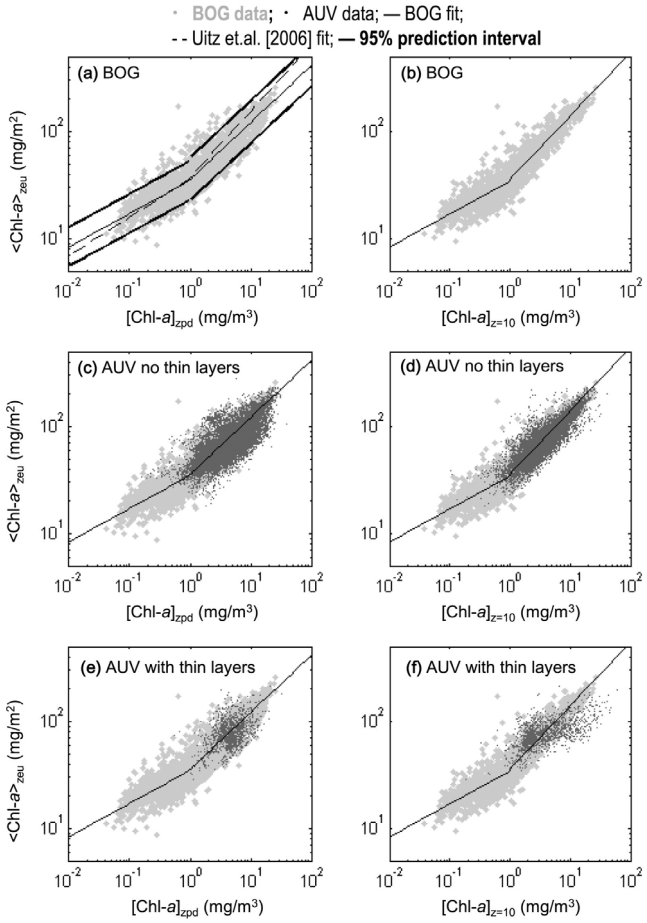

Figure 3. Predicting $\langle$Chl-$a\rangle_{zeu}$ based on (a, c, and e) [Chl-a]$_{zpd}$ and (b, d, and f) [Chl-a]$_{z=10}$. Figures 3c and 3d overlay points from the AUV data set (in black) for profiles without thin layers. Figures 3e and 3f overlay points from the AUV data set (in black) for profiles with thin layers.

over- or under-predicted observations by 50%; and RMSE of 2 means that the predicted value was on average twice larger (or smaller) than the observed value. Similar to RMSE error in equation (6), we computed bias in the prediction as

$$bias = 10\text{^}\left(mean\left[\log_{10}\left(\widehat{\langle \text{Chl-}a\rangle_{zeu}}\right) - \log_{10}\left(\langle \text{Chl-}a\rangle_{zeu}\right)\right]\right). \quad (7)$$

[20] To determine if the predicted values of $\langle$Chl-$a\rangle_{zeu}$ were statistically different for regression parameters estimated using data from the BOG database and estimated in *Uitz et al.* [2006], we used the two-sided t-test to compare the squares of prediction errors

$$\varepsilon^2_{bog} = \left(\log_{10}\left(\widehat{\langle \text{Chl-}a_{BOG}\rangle_{zeu}}\right) - \log_{10}\left(\langle \text{Chl-}a\rangle_{zeu}\right)\right)^2 \quad (8)$$

and

$$\varepsilon^2_{uitz} = \left(\log_{10}\left(\widehat{\langle \text{Chl-}a\rangle_{zeu}}\right) - \log_{10}\left(\langle \text{Chl-}a\rangle_{zeu}\right)\right)^2, \quad (9)$$

where ε^2_{bog} and ε^2_{uitz} are square errors computed for $\widehat{\langle \text{Chl-}a\rangle_{zeu}}$ concentrations predicted using regression parameters estimated from BOG and Uitz data sets respectively. If the statistics were different, we concluded that one regression model was more accurate and had significantly lower mean square of the prediction error.

3.3. Thin Layers

[21] To identify profiles with thin layers, we followed *Ryan et al.* [2010] and identified the profile of Chl-*a* fluorescence as having a thin layer if: (1) the intensity of the fluorescence peak was at least twice the background, (2) the width of the layer at full-width half-maximum was smaller than 3 m, and (3) a similar peak in the fluorescence and the backscatter profiles was present. The last criterion was used to ensure that the fluorescence profile structure is also a biomass maximum and not due to inhibition of chlorophyll fluorescence at high light intensities near the surface [*Cullen and Eppley*, 1981]. From the total of ~15,000 profiles in the AUV database, ~1500 profiles contained thin layers. In only 20% of cases, the thin layer maximum was within the first optical depth.

4. Results

4.1. Predicting $\langle$Chl-a$\rangle_{zeu}$ From Satellite-Observable [Chl-a]$_{zpd}$

[22] We found that open ocean relationships between [Chl-a]$_{zpd}$ and $\langle$Chl-$a\rangle_{zeu}$ could be effectively extended into high Chl-*a* waters of the CCCUE. Our data exhibited a similar piecewise linear relationship as *Morel and Berthon* [1989], with a change in slope at ~1 mg/m^3 (Figure 3a). Error statistics (equations (8) and (9)) for predicted $\widehat{\langle \text{Chl-}a\rangle_{zeu}}$ values show no significant differences ($p = 0.76$) between our regression parameters (Table 1) and those of *Uitz et al.* [2006] for [Chl-a]$_{zpd}$ concentrations less than 1 mg/m^3. However, error statistics do show significant differences ($p \ll 0.05$) for [Chl-a]$_{zpd}$ concentrations greater than 1 mg/m^3. These differences between the regression models can be clearly seen in Figure 3a, where the dashed line shows the relationship proposed by *Uitz et al.* [2006] and the solid line shows the relationship obtained in the present study. Our model had accuracy similar to that of *Uitz et al.* [2006], with the R^2 of 90% and RMSE of 1.22 times (dashed lines in Figures 4a and 4c). The confidence intervals for our model were the same as the model of *Uitz et al.*

Table 1. Parameters of the Regression in Equation (4) Fitted to the BOG Data Set of Chl-*a* Profiles in Stratified Waters[a]

Depth (m)	A		B		N (BOG)	
	<1 mg/m^3	>1 mg/m^3	<1 mg/m^3	>1 mg/m^3	<1 mg/m^3	>1 mg/m^3
zpd	35.0	35.9	0.310	0.530	1374	1461
0	35.9	37.6	0.299	0.488	1316	1306
5	34.9	35.5	0.299	0.559	1293	1340
10	34.5	35.9	0.308	0.591	1337	1472
15	34.7	38.6	0.327	0.611	1413	1414
20	39.5	44.7	0.391	0.543	1616	1214
25	41.1	48.7	0.386	0.528	1782	1018
30	43.9	51.5	0.359	0.464	1990	732

[a]A and B are regression parameters from equation (4). N is the number of samples used in the regression.

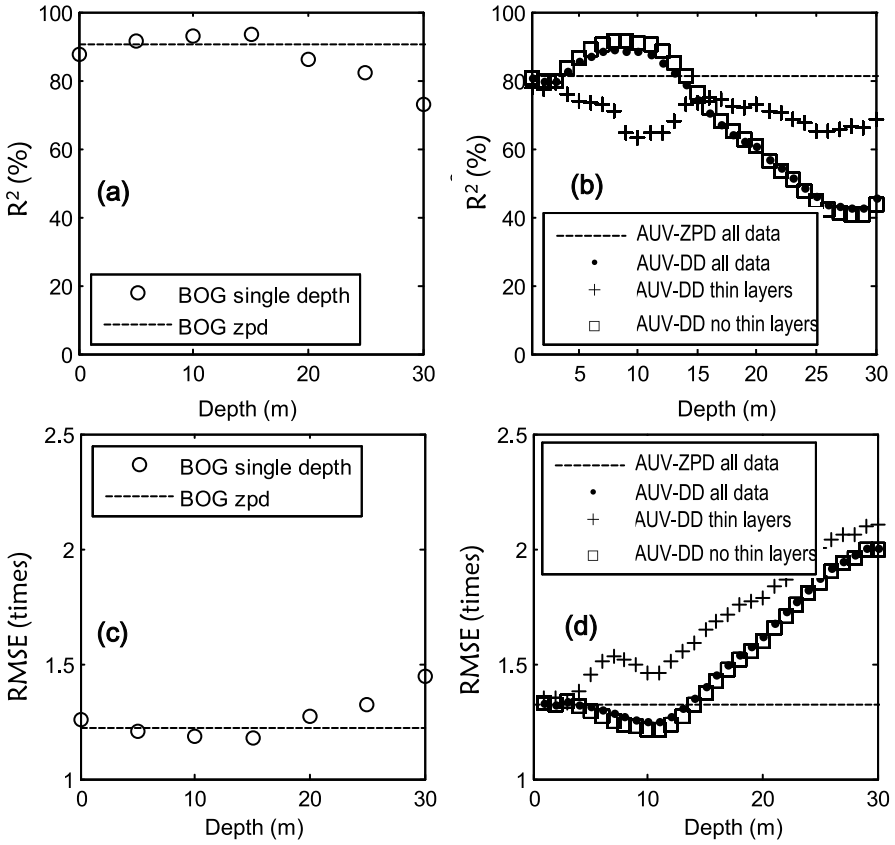

Figure 4. Error statistics for $\langle$Chl-$a\rangle_{zeu}$ prediction. (a) R^2 and (c) RMSE statistics for regressions trained and tested on the BOG data set. (b) R^2 and (d) RMSE statistics for regressions trained on the BOG data set and tested on the AUV data set. R^2 was computing using equation (5) and shows the percentage of the total variance explained by the regression model. RMSE was computed using equation (6) and shows the ratio by which predicted value over or under predicted observed values. AUV-ZPD stands for prediction of $\langle$Chl-$a\rangle_{zeu}$ from surface-integrated Chl-*a*: $[\text{Chl-}a]_{zpd}$. AUV-DD stands for prediction of $\langle$Chl-$a\rangle_{zeu}$ from a discrete-depth measurement of Chl-*a*: $[\text{Chl-}a]_z$.

[2006] for $[\text{Chl-}a]_{zpd}$ concentrations less than 1 mg/m^3, but were larger for $[\text{Chl-}a]_{zpd}$ concentrations greater than 1 mg/m^3. We explain higher noise for predictions above the 1 mg/m^3 threshold because our data set came from a wider variety of conditions than the data set used in *Uitz et al.* [2006] (compare the distribution of data points in our Figure 3a and the *Uitz et al.* [2006] Figure 3a).

[23] We found that the effect of thin layers on predictability of depth-integrated $\langle$Chl-$a\rangle_{zeu}$ from $[\text{Chl-}a]_{zpd}$ depended on vertical location of the layer. When the thin layer peaks were located below the first optical depth (z_{pd}), there was a minor bias toward underestimation of $\langle$Chl-$a\rangle_{zeu}$ (*bias* = 0.95 times, Figure 5a). When the thin layer peaks were located within the first optical depth, there was a major bias toward overestimation (*bias* = 1.4 times, Figure 5b).

4.2. Predicting $\langle$Chl-a$\rangle_{zeu}$ From Discrete-Depth $[\text{Chl-a}]_z$

[24] We found that, similar to the relationship between satellite-observable $[\text{Chl-}a]_{zpd}$ and depth-integrated $\langle$Chl-$a\rangle_{zeu}$, there was a strong relationship between discrete-depth $[\text{Chl-}a]_z$ and depth-integrated $\langle$Chl-$a\rangle_{zeu}$. For example, the shape of the relationship is the same between $\langle$Chl-$a\rangle_{zeu}$ and either $[\text{Chl-}a]_{zpd}$ (Figure 3a) or $[\text{Chl-}a]_{z=10}$ (Figure 3b). Furthermore, $[\text{Chl-}a]_z$ measurements taken between 5 and 15 m were slightly, yet statistically significant, better predictors of $\langle$Chl-$a\rangle_{zeu}$ than $[\text{Chl-}a]_{zpd}$ measurements (compare open circles and dashed line in the error statistics Figures 4a and 4c). Similar improvements were observed when we used AUV data to test regression models that were estimated using BOG data (compare dots with the dashed line in Figures 4b and 4d).

[25] We found that presence of thin layers had a large effect on the predictability of depth-integrated $\langle$Chl-$a\rangle_{zeu}$ from discrete-depth $[\text{Chl-}a]_z$ measurements. In profiles without thin layers (R^2 and RMSE values shown with squares in Figures 4b and 4d), the discrete-depth Chl-*a* concentrations measured between 4 and 13 m depth remained a better predictor of $\langle$Chl-$a\rangle_{zeu}$ than $[\text{Chl-}a]_{zpd}$ concentrations. However, for profiles with thin layers (R^2 and RMSE values shown with cross symbols in Figures 4b and 4d), the $[\text{Chl-}a]_z$ concentrations had lower predictive skill than $[\text{Chl-}a]_{zpd}$ (see divergence of box symbols and cross symbols between 3 and 15 m). Because in 95% of the cases the maximum Chl-*a* concentrations in the thin layer were located between 3.8 m and 13.6 m, we attribute this degraded skill to observing elevated Chl-*a* concentrations within a layer. Prediction based on elevated Chl-*a*

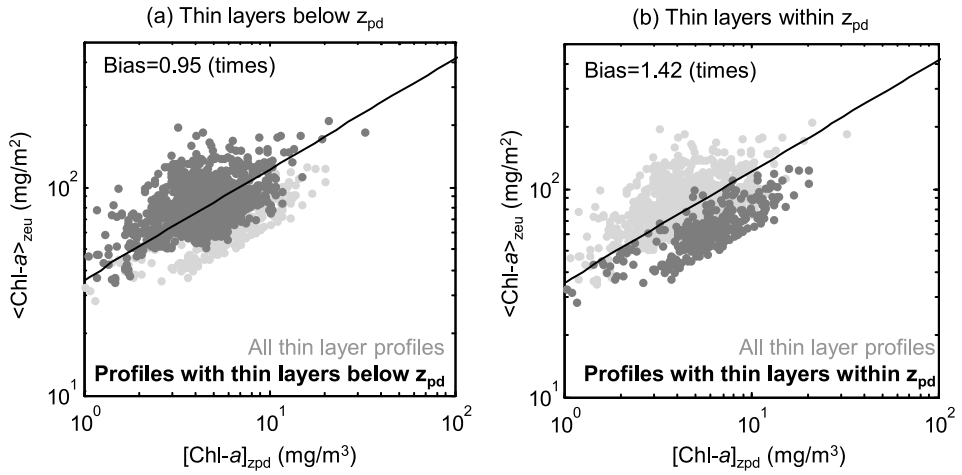

Figure 5. Effect of thin layer depth on $\langle$Chl-$a\rangle_{zeu}$ prediction. Prediction bias is computed using equation (7).

concentrations within a layer causes over-prediction of $\langle$Chl-$a\rangle_{zeu}$. This over-prediction can be seen in Figure 3f, where the regression model trained on observations of $[\text{Chl-}a]_{z=10}$ (black line) is biased high compared to the observed values of $\langle$Chl-$a\rangle_{zeu}$ (black dots).

5. Discussion

[26] Using an extensive data set of in situ Chl-*a* profiles in the CCCUE, we provided the first extensions of the open ocean relationships between $[\text{Chl-}a]_{zpd}$ and $\langle$Chl-$a\rangle_{zeu}$ to a coastal ecosystem. We found that despite differences in the trophic status and phytoplankton ecology, the functional shape of the relationship is the same. However, the regression parameters were different for the CCCUE and the open ocean model for $[\text{Chl-}a]_{zpd} > 1$ mg/m^3.

[27] The predictive relationships established in this paper have implications for the design of monitoring networks aimed at detecting the onset and the distribution of algal blooms in the CCCUE region:

[28] 1. The confirmed strong relationship between $\langle$Chl-$a\rangle_{zeu}$ and $[\text{Chl-}a]_{zpd}$ suggests that satellite-derived measurements of $[\text{Chl-}a]_{zpd}$ can be used effectively to locate areas with elevated levels of depth-integrated Chl-*a*.

[29] 2. The newly developed relationships between $[\text{Chl-}a]_z$ and $\langle$Chl-$a\rangle_{zeu}$ suggest that in situ Chl-*a* fluorometers deployed on moorings and underway sampling platforms are best located in the upper 15 m of the water column, with the optimal range between 5 and 10 m when no thin layers are present, and between 0 and 3 m when thin layers are present.

[30] 3. The robust predictive relationships for $\langle$Chl-$a\rangle_{zeu}$ established in this work suggest that satellite, moored, and underway measurements of Chl-*a* can be converted to a common reference quantity of the euphotic-depth-integrated Chl-*a*, which will promote synergistic use of these measurement platforms. In practice, these inter-platform comparisons will be contingent on further refinement of satellite retrieval algorithms for the coastal ocean [*Franz et al.*, 2006] and on the consistent calibration of in situ sensors.

[31] We found that the effect of thin layers on predictability of depth-integrated $\langle$Chl-$a\rangle_{zeu}$ from $[\text{Chl-}a]_{zpd}$ depended on vertical location of the layer. When thin layers were located within the first optical depth, predicted values of $\langle$Chl-$a\rangle_{zeu}$ were biased much higher than observed (1.42 times higher), reflecting elevated $[\text{Chl-}a]_{zpd}$ concentrations due to surface thin layers. Similar over-prediction was observed when we predicted $\langle$Chl-$a\rangle_{zeu}$ concentrations based on discrete $[\text{Chl-}a]_z$ measurements located between 4 and 13 depths—the range of depths where thin layer maxima typically occur. When thin layers were located below the first optical depth (z_{pd}), predictions of $\langle$Chl-$a\rangle_{zeu}$ based on satellite-observable $[\text{Chl-}a]_{zpd}$ were biased lower than observed, but only slightly (0.95 times lower). We interpret that the small magnitude of the bias is because when thin layers are present, they reduce the euphotic depth, which also reflects in a proportional reduction of the euphotic-depth-integrated $\langle$Chl-$a\rangle_{zeu}$.

[32] An outstanding question raised by this work is why the regression parameters that we established in the CCCUE region differed from the parameters documented by *Uitz et al.* [2006] for the open ocean. Were these differences due to differences in ecology or in data sets? We suspect that data sets may play a role because the CCCUE and open ocean parameters only differed for $[\text{Chl-}a]_{zpd}$ concentrations above the 1 mg/m^3 threshold, where the open ocean data set was very sparse. To answer this question definitively, it will be necessary to assemble a data set of similar quality that will include sufficient number of samples from the open ocean as well from more than one coastal system. With such a data set it should be possible to establish if a single relationship that works across the open ocean and coastal Case I waters is attainable.

[33] The results presented in this paper were developed for an upwelling coastal ecosystem, dominated by Case I ocean waters [*Morel et al.*, 2006]. Will similar relationships between $[\text{Chl-}a]_{zpd}$ and $\langle$Chl-$a\rangle_{zeu}$ hold in Case II waters? It is not possible to answer such a question without an extensive data set in Case II waters. However, we foresee that the methods that we used to compute euphotic depth Z_{eu} in Case I waters [*Morel and Berthon*, 1989] will need to be adjusted to account for absorption of light by non-algal matter, such as CDOM and suspended sediments.

[34] **Acknowledgments.** We are grateful to crew, lead scientists, engineers, and field technicians that collected and preserved three decades of ocean time series data. We would like to extend the specific gratitude to Tim Pennington and Reiko Michisaki for their help in preparation of the BOG data set, and the MBARI AUV operations team. SF is grateful for support, encouragement, and insightful discussions with James Bellingham. This work was supported by the David and Lucile Packard Foundation.

References

Cowles, T. J., R. A. Desiderio, and M. E. Carr (1998), Small-scale planktonic structure: Persistence and trophic consequences, *Oceanography*, *111*, 4–9.

Cullen, J. J., and R. W. Eppley (1981), Chlorophyll maximum layers of the Southern California Bight and possible mechanisms of their formation and maintenance, *Oceanol. Acta*, *4*, 23–32.

Cullen, J. J., and S. G. Horrigan (1981), Effects of nitrate on the diurnal vertical migration, carbon to nitrogen ratio, and the photosynthetic capacity of the dinoflagellate, Gymnodinium splendens, *Mar. Biol.*, *62*, 81–89, doi:10.1007/BF00388169.

Derenbach, J. B., H. Astheimer, H. P. Hansen, and H. Leach (1979), Vertical microscale distribution of phytoplankton in relation to the thermocline, *Mar. Ecol. Prog. Ser.*, *1*, 187–193, doi:10.3354/meps001187.

Franz, B. A., P. J. Werdell, G. Meister, E. J. Kwiatkowska, S. W. Bailey, Z. Ahmad, and C. R. McClain (2006), MODIS land bands for ocean remote sensing applications, paper presented at Ocean Optics XVIII, NASA, Montreal, Canada, 9–13 Oct.

Kiefer, D. A., and R. Lasker (1975), Two blooms of Gymnodinium splendens, an unarmoured dinoflagellate, *Fish. Bull.*, *73*, 675–678.

Lorbacher, K., D. Dommenget, P. P. Niiler, and A. Köhl (2006), Ocean mixed layer depth: A subsurface proxy of ocean-atmosphere variability, *J. Geophys. Res.*, *111*, C07010, doi:10.1029/2003JC002157.

McManus, M., R. M. Kudela, M. V. Silver, G. F. Steward, J. M. Sullivan, and P. L. Donaghay (2008), Cryptic blooms: Are thin layers the missing connection?, *Estuaries Coasts*, *31*, 396–401, doi:10.1007/s12237-007-9025-4.

Morel, A., and J.-F. Berthon (1989), Surface pigments, algal biomass profiles, and potential production of the euphotic layer: Relationships reinvestigated in view of remote-sensing applications, *Limnol. Oceanogr.*, *34*(8), 1545–1562, doi:10.4319/lo.1989.34.8.1545.

Morel, A., and S. Maritorena (2001), Bio-optical properties of oceanic waters: A reappraisal, *J. Geophys. Res.*, *106*(C4), 7163–7180, doi:10.1029/2000JC000319.

Morel, A., B. Gentili, M. Chami, and J. Ras (2006), Bio-optical properties of high chlorophyll Case 1 waters and of yellow-substance-dominated Case 2 waters, *Deep Sea Res., Part I*, *53*(9), 1439–1459, doi:10.1016/j.dsr.2006.07.007.

Pauly, D., and V. Christensen (1995), Primary production required to sustain global fisheries, *Nature*, *374*, 255–257, doi:10.1038/374255a0.

Pennington, J. T., and F. P. Chavez (2000), Seasonal fluctuations of temperature, salinity, nitrate, chlorophyll and primary production at station H3/M1 over 1989–1996 in Monterey Bay, California, *Deep Sea Res., Part II*, *47*, 947–973, doi:10.1016/S0967-0645(99)00132-0.

Ryan, J., M. A. McManus, and J. M. Sullivan (2010), Interacting physical, chemical and biological forcing of phytoplankton thin-layer variability in Monterey Bay, California, *Cont. Shelf Res.*, *30*(1), 7–16, doi:10.1016/j.csr.2009.10.017.

Sullivan, J., P. L. Donaghay, and J. Rines (2010a), Coastal thin layer dynamics: Consequences to biology and optics, *Cont. Shelf Res.*, *30*(1), 50–65, doi:10.1016/j.csr.2009.07.009.

Sullivan, J. M., et al. (2010b), Layered organization in the coastal ocean: An introduction to planktonic thin layers and the LOCO project, *Cont. Shelf Res.*, *30*(1), 1–6, doi:10.1016/j.csr.2009.09.001.

Uitz, J., H. Claustre, A. Morel, and S. B. Hooker (2006), Vertical distribution of phytoplankton communities in open ocean: An assessment based on surface chlorophyll, *J. Geophys. Res.*, *111*, C08005, doi:10.1029/2005JC003207.